Published in final edited form as:
Exp Eye Res. 2008 November ; 87(5): 415–426. doi:10.1016/j.exer.2008.07.016.

Rod Photoreceptor Differentiation in Fetal and Infant Human Retina

Anita Hendrickson[1], **Keely Bumsted-O'Brien**[2], **Riccardo Natoli**[2], **Visvanathan Ramamurthy**[3], **Daniel Possin**[1], and **Jan Provis**[2]

[1]Departments of Biological Structure and Ophthalmology, University of Washington, Seattle WA 98195

[2]Research School of Biological Sciences and ARC Centre of Excellence in Vision Science, Australian National University, Canberra, Australia

[3]Department of Ophthalmology, West Virginia University Health Center, Morgantown WV 26506

Abstract

Human rods and cones are arranged in a precise spatial mosaic that is critical for optimal functioning of the visual system. However, the molecular processes that underpin specification of cell types within the mosaic are poorly understood. The progressive differentiation of human rods was tracked from fetal week (Fwk) 9 to postnatal (P) 8 months using immunocytochemical markers of key molecules that represent rod progression from post-mitotic precursors to outer segment-bearing functional photoreceptors. We find two phases associated with rod differentiation. The early phase begins in rods on the foveal edge at Fwk 10.5 when rods are first identified, and the rod-specific proteins NRL and NR2e3 are detected. By Fwk 11-12, these rods label for interphotoreceptor retinoid binding protein, recoverin, and aryl hydrocarbon receptor interacting protein-like 1. The second phase occurs over the next month with the appearance of rod opsin at Fwk 15, closely followed by the outer segment proteins rod GTP-gated sodium channel and peripherin. TULP is expressed relatively late at Fwk 18-20 in rods. Each phase proceeds across the retina in a central-peripheral order, such that rods in far peripheral retina are only entering the early phase at the same time that cells in central retina are entering their late phase. During the second half of gestation rods undergo an intracellular reorganization of these proteins, and cellular and OS elongation which continues into infancy. The progression of rod development shown here provides insight into the possible mechanisms underlying human retinal visual dysfunction when there are mutations affecting key rod-related molecules.

Corresponding Author: Keely Bumsted O'Brien, Research School of Biological Sciences, GPO Box 475, The Australian National University ACT 2601, Ph: 02 6125 2389, Fax: 02 6125 8680, keely.bumsted-obrien@anu.edu.au.

Keywords

rod opsin; cone opsin; arrestin; NRL; NR2E3; peripherin; recoverin; AIPL1

Introduction

Human vision is functional over a wide range of light intensities by virtue of two light detection systems. Light capture occurs via a phototransduction molecule composed of a type-specific protein called opsin and 11-cis retinal. Vision under bright light is mediated by three types of cone photoreceptors. All cones absorb photons over a wide range of wavelengths, but in human retina each type contains an opsin which makes it optimally sensitive to long (L; 564nm), medium (M; 533nm) or short (S; 437nm) wavelength light so that the interaction of signals generated by these cones determines perceived color (Jacobs, 1996). In low level illumination, rod-mediated vision comes into play. Rods contain a single rod opsin (ROp) and are maximally sensitive to blue-green light (500nm). Unlike cones, dark adapted rods can detect a single photon of light (see (Rodieck, 1998)).

Human rods and cones are arranged in a precise spatial mosaic (Osterberg, 1935; Curcio et al., 1986; Curcio et al., 1990; Curcio et al., 1991). L&M cones reach peak spatial density in the center of the fovea while S cones are absent from the central 100μm and rods are absent from the central 300μm of the adult fovea. All four photoreceptor types occur outside the foveal center with rods reaching peak density at the eccentricity of the optic disc (Osterberg, 1935; Curcio et al., 1990). Outside the most central retina, rods greatly outnumber cones with a ratio of 1:20 (Curcio and Hendrickson, 1991). The generation and maintenance of this photoreceptor mosaic is critical for optimal functioning of the human visual system, but the precise molecules and processes underlying its creation are still poorly delineated (Provis et al., 1998; Hendrickson and Provis, 2006).

Gene defects in human rod photoreceptors are associated with numerous degenerative syndromes including retinitis pigmentosa, cone-rod dystrophy, Leber congenital amaurosis and Enhanced Short Wavelength Cone syndrome. Affected individuals can demonstrate a range of visual defects from complete loss of vision to night blindness or tunnel vision. In the cases where the genetic defect has been identified, many are associated with key genes in the development of the rod photoreceptor (www.sph.uth.tmc.edu/ Retnet). Mutations in ROp and the photoreceptor-specific tubby like protein (TULP) are associated with retinitis pigmentosa as well as a range of visual impairments (Banerjee et al., 1998; Lewis et al., 1999; Wilson and Wensel, 2003). Mutations in the visual transduction genes are associated with Stargart's disease while mutations in peripherin, the rod GTP-gated sodium channel (NaCh) and aryl hydrocarbon receptor interacting protein-like 1 (AIPL1) have been identified in patients with diffuse degeneration, macular degeneration, or Lebers congenital amaurosis (http://www.retina-international.com/sci-news/mutation.htm). The best studied genes for the specification and generation of rods are the Neural Retina Leucine Zipper (NRL) and NR2E3, a photoreceptor-specific orphan nuclear receptor. Missense mutations in NRL are associated with autosomal dominant retinitis pigmentosa (Bessant et al., 1999; Martinez-Gimeno et al., 2001; Wilson and Wensel, 2003). Mutations in NR2E3 are

associated with Enhanced Short-wavelength Cone Syndrome, an autosomal recessive retinal disorder characterized by an increased sensitivity to short wavelength light, color vision defects, an increased number of S opsin immunoreactive (-IR) cones, reduced or absent rod function and absence of ROp-IR rods (Jacobson et al., 1990; Hood et al., 1995; Greenstein et al., 1996; Haider et al., 2000; Milam et al., 2002). Taken together, these genes and disease conditions indicate that the proper temporal and spatial expression of many photoreceptor specific genes is absolutely critical to rod development and function.

Previous studies of primate retinal development agree that the fovea is the initiation point for most events, including cessation of mitosis (Provis et al., 1985), morphological maturation (Hendrickson and Yuodelis, 1984), apoptosis (Provis, 1987; Georges et al., 1999), opsin expression (Xiao and Hendrickson, 2000) and synaptogenesis (van Driel et al., 1990; Okada et al., 1994). A wave of differentiation for a specific developmental event is initiated at the site of the future fovea or pure cone area (PCA), and then spreads across the retina, reaching the retinal edges many weeks or months later. Given the long (40 week) gestation of humans and the large size of the retina, central regions are well developed at Fwk 20, while in peripheral regions the cells may be only beginning to exit the cell cycle. This allows a relatively “fine-grained” view of developmental events not possible in many experimental mammals which develop much more rapidly.

Surprisingly, despite their significance in visual disease, relatively little is known about rod development in the human retina. To further understand the aetiology and mechanism(s) of rod-based retinal degenerations, this paper will determine the sequence and cellular location in which human rod and associated photoreceptor genes are expressed.

Methods

Tissues and Processing

Human eyes were obtained with University of Washington (UW) Human Subject Committee approval (010447) through the UW Human Embryology Tissue Program, Neonatal Intensive Care Nursery and Lions Eye Bank, or through ABR, Inc. (San Mateo CA). Collection of donor retinas for *in situ* hybridization was co-ordinated by the Prince of Wales Hospital (Randwick, NSW, Australia) Department of Endocrinology, with informed consent and approval from the ANU human ethics committee. Ages sampled in this study ranged from Fwk 8-25; Fwk 34-37; postnatal (P) 1, 4 and 15 days; 4, 8 and 12 mo; 13, 45, 57 and 80yr. Retinas used for morphological analysis were fixed overnight in 4% paraformaldehyde/0.5% glutaraldehyde in 0.1M phosphate buffer, pH 7.4 followed by embedding in glycol methacrylate. Sections were cut serially at 2μm and stained with methylene blue/azure II in pH11.0 buffer.

In situ hybridization—Eyes used for ROp *in situ* hybridization were fixed overnight in 2% paraformaldehyde, rinsed and the anterior half removed. The eye cup was dehydrated in an ascending series of 0.1M phosphate buffer, pH 7.4 containing 0.1% Tween-20 (PBT) and methyl alcohol (MeOH), stored overnight at −20°C in absolute MeOH, and then rehydrated through a PBT/MeOH series. The retina and retina pigment epithelium were then dissected away from the sclera and any remaining pigment epithelium was bleached (Petry et al.,

1993; Hemmi and Grunert, 1999). *In situ* hybridization was carried out using digoxigenin-labeled ROp or NR2E3 riboprobes, as described previously (Bumsted et al., 1997; Bumsted and Hendrickson, 1999; Bumsted O'Brien et al., 2004; Cornish et al., 2004; Cornish et al., 2005)

Immunolabeling—Most eyes were fixed for 1-12 hrs in 2% paraformaldehyde, but some postnatal eyes were processed after being stored in 2% paraformaldehyde for months to years ('long fix'). All eyes were cryoprotected in 30% sucrose and cryosectioned serially at 10-20 μm parallel to the horizontal meridian. Every 10^{th} section was stained with azure II and methylene blue to identify the fovea, optic disc (OD) and retinal edges. Almost all sections in this study included or were immediately adjacent to the developing fovea. As far as possible, a series of adjacent sections from the same eye was immunolabeled for multiple markers so that their temporal expression could be compared at the same retinal locus.

Sections from 'long fix' retinas were treated overnight at 37°C with the antigen retrieval product Revealit (Immunosolutions.com) before processing. All sections were blocked for 1hour in 10% Chemiblocker (Chemicon, Tecaluma CA) in 0.01M phosphate buffered saline (PBS) containing 0.5% Triton X-100 and 0.05% sodium azide (diluent). Sections then were incubated overnight in a mixture of two primary antibodies diluted in 5% Chemiblocker in diluent. Rabbit polyclonal antisera were generated to the following antigens: purified AIPL; V. Ramamurthy, West Virginia Univ.; 1/1000); carboxy terminal 18 amino acids of human M opsin but this antiserum recognizes both M and L opsin (J. Saari, Univ.Washington; 1/2000); C terminal 33 amino acids of human S opsin (J. Nathans, Johns Hopkins Univ.; 1/15,000); full length human NRL (A. Swaroop, Univ.Michigan, 1/1000); full length human NR2E3 (A. Swaroop, 1/1000); recombinant human recoverin (Chemicon AB5585; 1/20,000), amino acids 287-296 of bovine rod arrestin (C. Craft, U.Southern California, 1/5000); and bovine rhodopsin (E.L. Kean, Case Western, 1/1000). Mouse monoclonal antisera were generated to the following antigens: amino acids 159-170 of the alpha subunit of human cone transducin (J. Hurley, Univ.Washington, 1/200); N terminal amino acids 2-39 of bovine rhodopsin (4D2, R. Molday,Univ. British Columbia; 1/250); rod GTP-gated sodium channel (R. Molday, Univ. British Columbia, 1/10); *Torpedo* synaptic vesicles (SV2, K. Buckley, Harvard; 1/800); alpha isoform of synaptophysin (Sigma S5768; 1/1000). A polyclonal antiserum was generated in rat to tubby-like protein 1 (TULP, P. Nishima, Jackson Laboratory, Bar Harbor ME). Sections were thoroughly washed and then incubated for one hour in a mixture of species-specific IgG tagged with Alexa488 (rabbit) and Alexa 594 (mouse or rat) 1/500 in diluent (Molecular Probes, Eugene OR), washed again and coverslipped. Antibody, dilutions and sources are given in Table 1. Retinal wholemounts were processed similarly, using the same antibody concentrations; only the times were extended to 3-5 days in primary, 2-3 days wash, and overnight in secondary antibody. Primary antibodies were omitted to serve as a negative control for all combinations of antibodies.

When a primary or secondary antibody was omitted, no labeling for the matching antibody was detected, indicating no cross reactivity between primary or secondary antibodies. Nonspecific 'background' labeling was low to absent for most antibodies. The exception was in the 'long fixed' retinas which had moderate levels of nonspecific labeling; several

monoclonal antibodies did not label in these retinas. To avoid misinterpretation based on fixation differences, labeling for each antibody was compared between sections of the same age but with different fixation times and any differences were noted. In addition, labeling for sets of antibodies at a given age was always done in adjacent sections in or near the PCA which will later be at the center of the adult fovea. All temporal comparisons for expression of a given protein only used data obtained from the same central retina region. To avoid confusion, mouse and rabbit antibodies to ROp are represented as red in all figures.

Sections and wholemounts were examined and photographed using a Nikon Optiphot fluorescence microscope equipped with narrow band pass filters (Omega Optical) to minimize “bleed through” of the fluorescence. Some figures were created by scanning Kodak E6 transparency film in a Microtek 2500F scanner using SilverFast AI software and then compiled using Adobe Photoshop CS2A. Digital images were acquired using a Zeiss Apotome microscope or a Zeiss LSM two-photon confocal microscope. Images were adjusted for color balance and sharpness using Adobe Photoshop CS2.

Results

Rods in Adult Retina

In adult central retina, antibodies to L&M opsin and ROp heavily label outer segments (OS; Fig. 1 A). In peripheral retina (Fig. 1B), rod OS are slightly longer and there is a lower density of cones and a higher density of rods than in central retina. Central cones are elongated compared with their counterparts in the periphery, so that they are of similar length as rod OS (Fig. 1A), but only about half the length of rod OS in the periphery (Fig. 1B). In all adult retinas, a few scattered rods have ROp labeled cell membranes. Arrestin immunoreactivity (Fig. 1C-D′, green) is present throughout the cytoplasm of the entire rod with the OS more lightly labeled (Fig. 1D). Peripherin is present in both rod and cone OS, but not the cytoplasm (Fig. 1 E, F). Recoverin labels the cytoplasm and OS in both rods and cones (Fig. 1G-G′). AIPL1 (not shown) labels rods, as reported previously (van der Spuy et al., 2003). Interphotoreceptor retinoid binding protein (IRBP; Fig. 1H-L, green) heavily labels the interphotoreceptor matrix around the OS and covers the IS as far as the outer limiting membrane (Fig. 1H, thin line). At higher magnification, double labeling for ROp and IRBP shows that both rod and cone OS have surface IRBP labeling (Fig. 1J-L). Double labeling for the rod GTP-gated sodium channel (NaCh) and ROp (Fig. 1O) shows NaCh labeling mainly on the surface membrane (Fig. 1M) while both the surface and disc membranes are ROp positive (Fig. 1O). Immunoreactivity for the rod nuclear markers NRL and NR2E3 is weak in adult retina (not shown).

Morphological Development of Rods

The incipient fovea can first be identified at Fwk 10.5-11 (Provis et al., 1985; Linberg and Fisher, 1990; Hendrickson, 1992; Xiao and Hendrickson, 2000) as a region <500μm in diameter, about 1500μm temporal to the optic disc. At this age it is the only retinal region which contains the five layers characteristic of the adult retina. The differentiated outer nuclear layer (ONL) is composed of a single layer of cones forming the PCA which will later be at the center of the adult fovea. The earliest rods (Fig. 2A, R) are present on the edge

of the Fwk 10.5-12 PCA as small, dense, oval nuclei wedged between the large, pale cone nuclei (Fig. 2A, C). Identifiable rods extend about 500μm towards the periphery (Fig. 2B) just beyond the point that an identifiable outer plexiform layer (OPL) disappears. In more peripheral retina, only cones can be identified morphologically (Fig. 2C).

At midgestation, the ONL on the edge of the PCA (Fig. 2D) contains a single outer layer of large pale cones underlain by a single layer of smaller dense rods. Central cone cell bodies are columnar with distinct synaptic pedicles which line the outer border of the OPL, while the inner border of the OPL is formed by a single layer of large pale horizontal cells. Rod somas lay on the inner aspect of the cone nuclei, have small cell bodies, dense nuclei, and narrow dense IS that extend beyond the outer limiting membrane into the subretinal space. The larger, thick cone IS also bulge into this space. It is difficult to identify OS on either photoreceptor type or synapses on rods or cones at this age, although antibody labeling shows that they clearly are present (see below). Near the Fwk 21 optic disc (Fig. 2E) the ONL contains a single layer of cones and 3-5 layers of densely packed rod somas. At 8.0 mm eccentricity in peripheral nasal retina (Fig. 2F), an intermittent band of cones and a thick band of densely packed rods forms the outer part of the outer neuroblastic layer. An irregular band of pale horizontal cells is present, but an OPL is not yet obvious.

In the weeks before birth, photoreceptor morphology becomes more mature across the entire retina. At Fwk 34, cones and rods near the PCA have OS (Fig.2G, arrows) and are forming elongated axons or fibers of Henle (fH), which terminate in distinct synaptic pedicles along the OPL (Fig.2G, arrowhead). Rod somas are packed two layers deep adjacent to the OPL, but rod spherules still cannot be identified morphologically. At the eccentricity of the optic disc at Fwk 34 (Fig.2H) there are up to 8 layers of rod somas, and both rod and cone IS and OS have undergone rapid maturation after midgestation (compare Fig. 2E with H). From late gestation into the postnatal period photoreceptors at the optic disc are longer and more mature looking than their counterparts within central retina (compare Fig. 2G and H) (Abramov et al., 1982; Hendrickson and Drucker, 1992; Dorn et al., 1995; Cornish et al., 2005). The retina has all adult layers at 8 mm eccentricity in the Fwk 34 nasal retina (Fig. 2J). Rod somas can be differentiated from cone somas and short IS and OS are present on both photoreceptor types. By Fwk 34, the OPL reaches to within 1mm of the nasal retinal edge, but the OPL does not appear at the temporal margin until Fwk 37.

In the early postnatal retina an immature fovea is present and there are more rods than cones on the PCA edge (Fig. 3A). At the optic disc (Fig. 3B) both rod and cone OS still are longer than those near the fovea. Maturation of photoreceptors in central retina gradually catches up so that by 8 months central OS are longer than those at the optic disc (Fig. 3C). Packing of cones and rods during foveal development creates long fH on central photoreceptors (Yuodelis and Hendrickson, 1986). Peripheral rod OS are much longer by 8mo (Fig. 3D). By 5 years (not shown) the retina appears mature.

Spatial and Temporal Expression of Rod Proteins

For the proteins investigated here, expression occurred in two phases – (1) before expression of ROp (AIPL1, recoverin, IRBP, NRL and NR2E3), and (2) coincident, or just after ROp (arrestin, peripherin, NaCh, and TULP).

Early Phase: Onset of rod protein expression—No immunoreactivity was detected for rod markers before Fwk 10.5-11. This was not a defect in the tissue or methodology since cones in the PCA at Fwk 9-10 label for recoverin, IRBP, cone transducin, synaptophysin and synaptic vesicle protein 2 (SV2).

At Fwk 11 NRL- and NR2E3-IR nuclei are present on the edge of the PCA out to ∼750μm eccentricity, with a few labeled rods scattered within the PCA. In double labeled sections, NRL-IR and NR2e3-IR rod nuclei were located below and between cone transducin-IR cell bodies (Fig. 4 A-B). AIPL1 labeled both rods and cones at this age (Fig. 4C) with both the cytoplasm and nuclei AIPL1-IR. Some rods on the margin of the PCA were recoverin-IR although these were more common at Fwk 12-13. Scattered IRBP-IR rods were detected on the PCA edge on the inner side of IRBP-IR /SV2-IR cones at Fwk 13 (Fig. 4D) with both the nucleus and cytoplasm labeled for IRBP. This sequence on the PCA edge suggests that NRL and NR2E3 slightly precede IRBP and recoverin expression in rods.

By Fwk 14-15 all of the early expressed rod markers are present into the midperiphery (Fig. 4E-F), although the labeled rods at Fwk 14 were only 3 deep (Fig 4E-F) compared to 9-12 deep by Fwk 18 (Fig. 4H). Some NRL-IR rods are aligned in rows on the inner aspect of a thick band of NRL immunoreactivity (Fig.4H, arrow), and ectopic cells expressing rod or cone markers also are seen in the inner retina (Fig. 4 E,F, arrows). These ectopic cells appear and disappear in a wave following expression of the early rod markers. An increase in ONL thickness and presence of ectopic photoreceptors suggests that rods are still being generated in the peripheral retina close to midgestation. In comparison, peripheral cones at this age are synaptophysin- and SV2-IR (Fig.4F), even though the OPL does not form in the periphery until after Fwk 20 (Fig. 2F). Cones and the inner plexiform layer (IPL) label for these synaptic markers throughout central retina at Fwk 14-15 (Fig. 4G), but rod synaptic label is not obvious. IRBP only transiently is present in both rod and cone cell bodies and then rapidly disappears, simultaneous with increased IRBP labeling in the interphotoreceptor matrix (not shown). The intensity of nuclear labeling for NRL and NR2E3 reaches a peak about 6-8 weeks after these markers are first expressed, and then declines with increasing age, so that it is almost absent over much of the neonatal retina (not shown).

Late Phase: Onset of ROp Expression

***In situ* Hybridization for ROp mRNA:** In situ hybridization for NR2E3 mRNA shows a solid ring of rods around the PCA at Fwk 16 (Fig. 5A), indicating central rod fate has been determined (for discussion see (Bumsted O'Brien et al., 2004)). The earliest expression of ROp mRNA was detected in scattered, isolated cells near the PCA at Fwk 14 (not shown). By Fwk 15, rod expressing ROp mRNA were detected out to ∼1 mm eccentricity (Fig. 5B) with little evidence for clusters of labeled cells. Scattered rods expressing NR2E3 and ROp mRNA were present within the PCA (Fig. 5A, arrowheads). By Fwk 18 most rods around the PCA expressed ROp mRNA and the most peripheral were at ∼2 mm eccentricity. ROp mRNA expression was detected in rods near the optic disc by Fwk 20-21.

ROp Immunoreactivity: Double labeling of sections for ROp mRNA and protein showed mRNA expression in the IS of rods (Fig. 5C red, arrowhead) and short ROp-IR OS (Fig. 5C,

green, arrow). Messenger RNA was detected in rods approximately 1mm farther peripheral than protein, indicating mRNA is expressed about 1week before protein.

ROp-IR in sections and retinal wholemounts showed the same spatial pattern of onset of expression as observed for mRNA, with no-IR rods detected before Fwk 15. At Fwk 16 about half of the NRL labeled nuclei (Fig. 5D, arrowhead) on the edge of the PCA had ROp localized to the cytoplasm and cell membranes (Fig. 5D, arrow). Sections showed that in individual rods, ROp labeling was first detected in the cilium/OS (Fig. 5E, arrowhead), then in the entire rod cell membrane (Fig. 5E, arrow), as previously described for primate rod and cone opsins (Dorn et al., 1995; Bumsted et al., 1997; Xiao and Hendrickson, 2000). ROp immunoreactivity in the cell membrane persists for 1-2 months (Fig. 6A), and then with age in most rods becomes confined to the lengthening OS. Scattered rod cell bodies label even after birth (Fig. 8F-K).

The opsin expression sequence for L&M opsin and ROp was most clearly seen by double labeling of retinal wholemounts. At Fwk 15 (Fig. 6B) an initial and approximately simultaneous onset of opsin expression was found in rods and cones within and around the PCA. Even at this initial stage, there were many more labeled cones (n=62) compared to rods (n=37), establishing a pattern to be found across the retina. In two wholemounts from a single Fwk 16.7 donor, the PCA was densely filled with L&M-IR cones (Fig. 6D) with this region clearly outlined by ROp-IR rods (Fig. 6C,E), and S opsin-IR cones (Fig. 6F). The rod free zone measured 680μm in diameter while the S cone free zone was about 300-340 μm in diameter similar to Bumsted and Hendrickson (1999). Both are larger than in the adult, but relative to each other their proportions are similar. Scattered ROp-IR and S opsin-IR cells are still seen throughout the Fwk 16.7 PCA. In a specimen at Fwk 22 (Fig. 6G) the number of labeled rods around the PCA had increased dramatically, the rod-free zone was 1mm in diameter, and the PCA contained almost no rods. After Fwk 17, the onset of ROp-IR slowly spread from central retina in centro-peripheral order (Fig. 6H, J). The exception to this pattern appeared as the expression front reached and crossed the optic disc. ROp positive rods first appeared on the temporal side of the optic disc at Fwk 18, although the ROp expression front was still 500-1000μm away, and a ring of labeled rods surrounded the optic disc (Fig. 6K). The ROp expression wave had crossed the disc by Fwk 22-24.

Despite the 20:1 numerical dominance of rods across most of the adult retina, there were always more L&M-IR cones than ROp-IR rods at the expression front, and L&M-IR cones could be detected farther into peripheral retina (Fig. 6H-J; Fig. 7A-F). These differences in onset can be seen in the Fwk 25 expression front (Fig 7A-F) when both opsins extend ∼3 mm into nasal retina beyond the optic disc. At the optic disc (Fig. 7A) and just nasal to the disc (Fig. 7B), most cones are L&M positive. At the expression front (Fig. 7C) clusters of cones are labeled, and scattered L&M-IR cones can be detected 1.5mm further into the periphery (not shown). Most rods at the optic disc are immunoreactive (Fig. 7D), but labeling drops off markedly just nasal to the disc (Fig. 7E) and very few ROp-IR rods are found at the expression front (Fig. 7F). This pattern confirms that L&M opsin is expressed before ROp across the retina. Labeled rods and cones were detected near the nasal retinal edge by Fwk 34-36, and near the temporal edge at Fwk 40 (birth).

At birth, the central retina is densely packed with ROp-IR rods and L&M-IR cones, both with elongated OS (Fig. 7G). In contrast, there are relatively few photoreceptors in the far periphery and these have very short OS (Fig. 7H,J) suggesting that many photoreceptors in the far periphery are either not expressing ROp at birth, or have not yet been specified. Large numbers of ectopic ROp-IR cells are found in the INL throughout retinas in the perinatal period (Fig. 7G), suggesting that rod generation continues after birth in humans, especially in the periphery.

Late Phase: Onset of phototransduction and structural proteins— Immunoreactivity for peripherin (Fig. 8A, B), arrestin (Fig. 8D-G) and NaCh (Fig. 8H-L) is closely associated with the onset of ROp-IR. Peripherin is first detected at Fwk 15-16 in both rod and cone OS (Fig. 8A,B respectively). At the opsin expression front only ROp-IR OS contain peripherin labeling, indicating peripherin is expressed simultaneously with ROp. Cell membrane or cytoplasmic labeling for peripherin is absent at all ages. Arrestin is first detected in the cytoplasm and OS at Fwk 15-16, with most of the OS double labeled (Fig. 8D-E, arrows). By birth, arrestin-IR becomes heavier in the rod cytoplasm (Fig. 8F-G). NaCh also is first detected at Fwk 15-16 on the edge of the PCA (Fig. 8H-J). Some ROp-IR OS do not express NaCh, suggesting that NaCh protein appears slightly after opsin. NaCh immunoreactivity increases as rod OS lengthen after birth (Fig. 8K-L).

TULP is the last rod protein to appear. It first is detected in the cytoplasm of a few rods around the PCA at Fwk 18, about 3 weeks after ROp first appears. By Fwk 20-22 many rods in central retina have intense TULP protein localization in their cytoplasm which is retained into infancy, but rod OS labeling is light to absent for TULP throughout fetal life (Fig. 8C).

Discussion

In this study we describe development of the rod photoreceptor population and expression of key rod-associated proteins in the human retina. Our results suggest two phases of rod differentiation, each of which occurs first in the rods on the PCA edge. The first or early phase involves *generation and specification* of rods which begins around Fwk 11 and is marked by expression of rod-specific NRL and NR2e3. Other photoreceptor-associated proteins including AIPL1, recoverin and IRBP appear in rods over the next month. The second or later stage of rod *differentiation and maturation* begins at Fwk15, when both ROp mRNA and protein begin to be expressed. Proteins associated with visual transduction in the OS, including arrestin, NaCh and peripherin, are expressed at Fwk 15-16, with TULP the last to appear at Fwk 17. This later phase of differentiation extends over many months. During this time there is re-arrangement of cellular proteins and rods develop an adult-like elongated morphology, a synaptic spherule and a very long OS. Both phases proceed in central-peripheral order, with the late phase of maturation not initiated at the retinal edge until around birth. A summary of the expression sequence for proteins in human rods is provided in Figure 9.

Developmental Gradients of Rod Opsin Expression

In total, four exceptions to the dogma of a ‘central to peripheral’ wave of differentiation in the retina were observed in this study. Two of these exceptions have previously been noted

in humans and monkeys; (1) the late maturation of foveal cones, and (2) the lag in parafoveal rod OS elongation (Abramov et al., 1982; Hendrickson and Yuodelis, 1984; Hendrickson and Drucker, 1992; Dorn et al., 1995; Cornish et al., 2005). Two additional exceptions have been identified in this study. First is the early expression of ROp around the optic disc ahead of the oncoming ROp expression front. This early expression of ROp is possibly related to differences in the local environment at the disc, including increased vascularity, higher tissue $P0_2$, and elevated growth factor concentrations (Bowers et al., 2001) which may promote ROp expression in the local environment. However, no similarly precocious expression of cone opsins has been detected in either macaque or human retina (Bumsted and Hendrickson, 1999; Xiao and Hendrickson, 2000). We also observed that once ROp expression is present throughout central retina, rods near the optic disc elaborate OS faster than the more central rods, suggesting that this pattern of precocious development of rods at the disc is prolonged. These findings are consistent with testing of rod sensitivity in 10 week human infants, which shows greater rod sensitivity at 30° eccentricity (nasal) than at 10° / ∼2 mm from the fovea (Hansen and Fulton, 1995). At 10 weeks rhodopsin content is approximatey 50% adult levels, which are reached by 3 years of age (Fulton et al., 1999). These, along with the present data suggest that, although OS length or ROp protein labeling is a relatively coarse measure, it is reasonable predictor of rod function.

Second, we found a progressive reduction in the number of NRL-IR and ROp containing cells from the PCA after Fwk 20, suggesting that early in development a small number of rods are specified and express ROp within the PCA which are eliminated before the PCA becomes specialized further. Similarly, S cones are found scattered throughout the PCA of human retina between Fwk13-20, but are virtually absent thereafter (Bumsted and Hendrickson, 1997;1999; Xiao and Hendrickson, 2000)

Rod Generation, Differentiation and Maturation in the Human Retina

Because it is not possible to carry out birth-dating studies in humans we do not know the exact time when the first rods are generated. Birth-dating using tritiated thymidine in Macaque monkeys (LaVail et al., 1991) shows that rods located on the edge of the PCA are generated around fetal day (Fd) 43-45, 10 days after the first cones are generated. Morphologically, rods can be recognized on the PCA edge in monkey retina by Fd 47 (Hendrickson, 1992), indicating that the interval between their last cell division and taking up their position in the ONL is 2-5 days. Viewed as a proportion of the caecal period (CP) (Dreher and Robinson, 1988), rods in macaque retina are born at 25% CP and are identifiable morphologically at 27% CP on the edge of the fovea. Many landmarks in development of human and macaque retinas occur at similar stages of the CP (Hendrickson and Provis, 2006). Extrapolation from the CP data from macaque predicts that in humans the first rods are generated at around Fwk 10, and are recognizable on the edge of the PCA by Fwk 10.8, consistent with our present findings. Further comparison of the present findings with the data from macaque, in which rods reach their adult length by 1 year of age, we estimate that human rod OS elongate until at least 4 years postnatal.

The early phase of rod generation and specification moves rapidly across the retinareaching the midperiphery by Fwk 14, and far periphery by Fwk 18. As this wave of differentiation

passes, the ONL becomes thicker and there is a gradual increase in rod OS numbers. This increase in ONL thickness and OS number continues in the periphery until about 8 months after birth (Xiao and Hendrickson, 2000). We also observed in this study cells that express rod markers located in the INL or GCL, at Fwk 14-16 in central retina and in the far periphery in the perinatal period. These could be either rods that migrate incorrectly, or which are late-generated cells from rod progenitors located in the INL, as described in fish retina (Raymond and Rivlin, 1987). Our findings are consistent with recent work indicating that a population of stem and/or progenitor cells remains in the far periphery of mature mammalian retinas, including primates (Reh and Fischer, 2006; Lawrence et al., 2007), and suggest that rods may be added to the periphery of human retina for many years after birth.

Rod *vs.* Cone Differentiation

Birth-dating studies in monkeys and other mammals show that at a given retinal location, cone populations are generated earlier than rods. The present study shows that despite this difference in timing, all post-mitotic photoreceptor progenitors express recoverin, IRBP and AIPL1 prior to opsin. Cells destined to a rod fate express NRL and NR2E3 before they express rod opsin (Mears et al., 2001; Swain et al., 2001; Bumsted O'Brien et al., 2004, present study). However, TULP and AIPL1 do not follow the stereotypical pattern for photoreceptor markers. TULP has been shown to label only cones at Fwk 9-10 in the developing PCA (Milam et al., 2000). In this study we find that by Fwk 17-18, a subset of rods around the PCA also express TULP *after* the onset of ROp expression (Fig. 9). We also find that while AIPL1 is expressed during early retinal development by both rods *and* cones (Fig. 4B,F,K) over time it becomes restricted to the rod population (data not shown; (van der Spuy et al., 2003)). The functional significance of these changes in expression, however, is not clear.

A significant difference in the maturation of rods and cones concerns the relationship between opsin expression and synapse formation. Opsin expression in newly differentiated cones is delayed by approximately 7 weeks in humans and 35 days in macaques (LaVail et al., 1991; Bumsted et al., 1997; Xiao and Hendrickson, 2000). During this period there is an onset of synaptic and neurotransmitter protein expression in cones, accompanied by synapse formation (Linberg and Fisher, 1990; Okada et al., 1994; Georges et al., 1999; Nag and Wadhwa, 2001). By comparison, we have found little evidence, in this and in previous studies (Dorn et al., 1995; Bumsted O'Brien et al., 2003; Bumsted O'Brien et al., 2004), of rod synapse formation by rods until *after* ROp expression. Early electron microscopic studies also noted that at a given point in peripheral retina, cone pedicles contained synaptic vesicles and ribbons 2-3 weeks before the first rod spherules (Hollenberg and Spira, 1973). Together, these findings indicate human rods form synaptic contacts only *after* they express ROp, unlike cones in which synapse formation begins approximately 3 weeks prior to expression of L/M opsin (Xiao and Hendrickson, 2000).

Based simply on the present findings it is tempting to speculate that early expression of rod specific NRL and NR2E3 at Fwk 12 allows a subset of cone progenitors to express S opsin at Fwk12, then rods and L&M cones to express opsins at Fwk15. However, examination of the sequences of opsin expression in Macaque monkey retina (Dorn et al., 1995; Bumsted et

al. 1997) and New World marmoset monkey indicates that the sequence of opsin expression is not fixed. While in humans as the expression front moves across the retina, S opsin is expressed first at Fwk 12, followed by ROp and L/M opsin at Fwk 15 in the central region (Xiao and Hendrickson, 2000; Bumsted O'Brien et al., 2003), in Macaques ROp is expressed first, closely followed by S opsin, with L&M opsin significantly lagging (Bumsted et al., 1997). In marmosets, ROp is expressed first, closely followed by L&M opsin, with S opsin being the *last* opsin expressed at any given location (Hendrickson, in preparation). These different opsin expression patterns strongly argue against any marked temporal or spatial interactions between primate photoreceptors to initiate opsin expression.

Development in Relation to Disease Phenotype

The progression of rod development shown here provides further insight into possible mechanisms underlying human retinal visual dysfunction. We know that in early-onset diseases, where a gene is missing or defunct, there is a high probability that rod or cone fate is affected causing visual impairment that is manifest in early childhood. For example, in Enhanced S cone Syndrome there is a defect in the NR2E3 gene, and rods appear to be switched to an S cone fate (Milam et al., 2002). Similarly, in thyroid receptor beta 2 deficient mice, M cones are switched to an S cone fate (Ng et al., 2001). In contrast, mutations in genes that make up or maintain the OS structure or function lead to retinal degenerations that are slower in onset as is the case with peripherin or opsin mutations (Bentrop, 1998; Wilson and Wensel, 2003; Goldberg, 2006). By understanding the details of rod development and the sequence of protein assembly in their OS, we gain further insight into diseases affecting rod function and survival.

Acknowledgments

The authors would like to thank the ARC Centre of Excellence in Vision Science for providing funding for this work. This work was supported in part by resources of the Vision CORE EY01730 at the University of Washington and The Ophthalmic Research Institute of Australia.

References

Abramov I, Gordon J, Hendrickson A, Hainline L, Dobson V, LaBossiere E. The retina of the newborn human infant. Science. 1982; 217:265–267. [PubMed: 6178160]

Banerjee P, Kleyn PW, Knowles JA, Lewis CA, Ross BM, Parano E, Kovats SG, Lee JJ, Penchaszadeh GK, Ott J, Jacobson SG, Gilliam TC. TULP1 mutation in two extended Dominican kindreds with autosomal recessive retinitis pigmentosa. Nat Genet. 1998; 18:177–179. [PubMed: 9462751]

Bentrop J. Rhodopsin mutations as the cause of retinal degeneration. Classification of degeneration phenotypes in the model system Drosophila melanogaster. Acta Anatomica. 1998; 162:85–94. [PubMed: 9831754]

Bessant DA, Payne AM, Mitton KP, Wang QL, Swain PK, Plant C, Bird AC, Zack DJ, Swaroop A, Bhattacharya SS. A mutation in NRL is associated with autosomal dominant retinitis pigmentosa. Nat Genet. 1999; 21:355–356. [PubMed: 10192380]

Bowers F, Valter K, Chan S, Walsh N, Maslim J, Stone J. Effects of oxygen and bFGF on the vulnerability of photoreceptors to light damage. Investigative Ophthalmology & Visual Science. 2001; 42:804–815. [PubMed: 11222544]

Bumsted K, Hendrickson A. Human and Maccaca monkey retinas show different developmental patterns for S-cone distribution. Investigative Ophthalmology and Visual Science. 1997; 38(Supplement):S30.

Bumsted K, Jasoni C, Szel A, Hendrickson A. Spatial and temporal expression of cone opsins during monkey retinal development. Journal of Comparative Neurology. 1997; 378:117–134. [PubMed: 9120051]

Bumsted K, Hendrickson A. Distribution and development of short-wavelength cones differ between Macaca monkey and human fovea. Journal of Comparative Neurology. 1999; 403:502–516. [PubMed: 9888315]

Bumsted O'Brien KM, Schulte D, Hendrickson AE. Expression of photoreceptor-associated molecules during human fetal eye development. Molecular Vision. 2003; 9:401–409. [PubMed: 12949469]

Bumsted O'Brien KM, Cheng H, Jiang Y, Schulte D, Swaroop A, Hendrickson AE. Expression of Photoreceptor-Specific Nuclear Receptor NR2E3 in Rod Photoreceptors of Fetal Human Retina. Invest Ophthalmol Vis Sci. 2004; 45:2807–2812. [PubMed: 15277507]

Cornish EE, Natoli RC, Hendrickson A, Provis JM. Differential distribution of fibroblast growth factor receptors (FGFRs) on foveal cones: FGFR-4 is an early marker of cone photoreceptors. Molecular Vision. 2004; 10:1–14. [PubMed: 14737068]

Cornish EE, Madigan MC, Natoli RC, Hales A, Hendrickson A, Provis JM. Gradients of cone differentiation and FGF expression during development of the foveal depression in macaque retina. Visual Neuroscience. 2005; 22:447–459. [PubMed: 16212702]

Curcio CA, Sloan KR, Hendrickson AE, Kalina RE. Individual variability in topography of human retinal photoreceptors. Society for Neuroscience Abstracts. 1986; 12:636.

Curcio CA, Allen KA, Sloan KR, Lerea CL, Hurley JB, Klock IB, Milam AH. Distribution and morphology of human cone photoreceptors stained with anti-blue opsin. Journal of Comparative Neurology. 1991; 312:610–624. [PubMed: 1722224]

Curcio CA, Hendrickson A. Organization and development of the primate photoreceptor mosaic. Progress in Retinal Research. 1991; 10:90–120.

Curcio CE, Sloan KR, Kalina RE, Hendrickson A. Human photoreceptor topography. Journal of Comparative Neurology. 1990; 292:497–523. [PubMed: 2324310]

Dorn EM, Hendrickson L, Hendrickson AE. The appearance of rod opsin during monkey retinal development. Investigative Ophthalmology & Visual Science. 1995; 36:2634–2651. [PubMed: 7499086]

Dreher B, Robinson SR. Development of the Retinofugal Pathway in Birds and Mammals: Evidence for a common ‘timetable’. Brain, Behaviour and Evolution. 1988; 31:369–390.

Fulton AB, Dodge J, Hansen RM, Williams TP. The rhodopsin content of human eyes. Invest Ophthalmol Vis Sci. 1999; 40:1878–1883. [PubMed: 10393065]

Georges P, Madigan MC, Provis JM. Apoptosis during development of the human retina: relationship to foveal development and retinal synaptogenesis. Journal of Comparative Neurology. 1999; 413:198–208. [PubMed: 10524333]

Goldberg AF. Role of peripherin/rds in vertebrate photoreceptor architecture and inherited retinal degenerations. Int Rev Cytol. 2006; 253:131–175. [PubMed: 17098056]

Greenstein VC, Zaidi Q, Hood DC, Spehar B, Cideciyan AV, Jacobson SG. The enhanced S cone syndrome: an analysis of receptoral and post-receptoral changes. Vision Res. 1996; 36:3711–3722. [PubMed: 8977001]

Haider NB, Jacobson SG, Cideciyan AV, Swiderski R, Streb LM, Searby C, Beck G, Hockey R, Hanna DB, Gorman S, Duhl D, Carmi R, Bennett J, Weleber RG, Fishman GA, Wright AF, Stone EM, Sheffield VC. Mutation of a nuclear receptor gene, NR2E3, causes enhanced S cone syndrome, a disorder of retinal cell fate. Nat Genet. 2000; 24:127–131. [PubMed: 10655056]

Hansen RM, Fulton AB. Dark-adapted thresholds at 10- and 30-deg eccentricities in 10-week-old infants. Vis Neurosci. 1995; 12:509–512. [PubMed: 7654607]

Hemmi JM, Grunert U. Distribution of photoreceptor types in the retina of a marsupial, the tammar wallaby (Macropus eugenii). Vis Neurosci. 1999; 16:291–302. [PubMed: 10367964]

Hendrickson A. A morphological comparison of foveal development in man and monkey. Eye. 1992; 6:136–144. [PubMed: 1624035]

Hendrickson A, Drucker D. The development of parafoveal and mid-peripheral human retina. Behavioural Brain Research. 1992; 49:21–31. [PubMed: 1388798]

Hendrickson, A.; Provis, J. Comparison of development of the primate fovea centralis with peripheral retina. Sernagor, E.; Eglen, SJ.; Harris, WA.; Wong, RO., editors. Retinal Development, Cambride University Press; Cambridge: 2006.

Hendrickson AE, Yuodelis C. The morphological development of the human fovea. Ophthalmology. 1984; 91:603–612. [PubMed: 6462623]

Hollenberg MJ, Spira AW. Human retinal development: ultrastructure of the outer retina. American Journal of Anatomy. 1973; 137:357–385. [PubMed: 4730460]

Hood DC, Cideciyan AV, Roman AJ, Jacobson SG. Enhanced S cone syndrome: evidence for an abnormally large number of S cones. Vision Res. 1995; 35:1473–1481. [PubMed: 7645276]

Jacobs GH. Primate photopigments and primate color vision. Proceedings of the National Academy of Sciences of the United States of America. 1996; 93:577–581. [PubMed: 8570598]

Jacobson SG, Marmor MF, Kemp CM, Knighton RW. SWS (blue) cone hypersensitivity in a newly identified retinal degeneration. Invest Ophthalmol Vis Sci. 1990; 31:827–838. [PubMed: 2335450]

LaVail MM, Rapaport DH, Rakic P. Cytogenesis in the monkey retina. Journal of Comparative Neurology. 1991; 309:86–114. [PubMed: 1894769]

Lawrence JM, Singhal S, Bhatia B, Keegan DJ, Reh TA, Luthert PJ, Khaw PT, Limb GA. MIO-M1 cells and similar muller glial cell lines derived from adult human retina exhibit neural stem cell characteristics. Stem Cells. 2007; 25:2033–2043. [PubMed: 17525239]

Lewis CA, Batlle IR, Batlle KG, Banerjee P, Cideciyan AV, Huang J, Aleman TS, Huang Y, Ott J, Gilliam TC, Knowles JA, Jacobson SG. Tubby-like protein 1 homozygous splice-site mutation causes early-onset severe retinal degeneration. Invest Ophthalmol Vis Sci. 1999; 40:2106–2114. [PubMed: 10440267]

Linberg KA, Fisher SK. A burst of differentiation in the outer posterior retina of the eleven-week human fetus: an ultrastructural study. Visual Neuroscience. 1990; 5:43–60. [PubMed: 2271459]

Martinez-Gimeno M, Maseras M, Baiget M, Beneito M, Antinolo G, Ayuso C, Carballo M. Mutations P51U and G122E in retinal transcription factor NRL associated with autosomal dominant and sporadic retinitis pigmentosa. Hum Mutat. 2001; 17:520. [PubMed: 11385710]

Mears AJ, Kondo M, Swain PK, Takada Y, Bush RA, Saunders TL, Sieving PA, Swaroop A. Nrl is required for rod photoreceptor development. Nat Genet. 2001; 29:447–452. [PubMed: 11694879]

Milam AH, Hendrickson AE, Xiao M, Smith JE, Possin DE, John SK, Nishina PM. Localization of tubby-like protein 1 in developing and adult human retinas. Invest Ophthalmol Vis Sci. 2000; 41:2352–2356. [PubMed: 10892883]

Milam AH, Rose L, Cideciyan AV, Barakat MR, Tang WX, Gupta N, Aleman TS, Wright AF, Stone EM, Sheffield VC, Jacobson SG. The nuclear receptor NR2E3 plays a role in human retinal photoreceptor differentiation and degeneration. Proc Natl Acad Sci U S A. 2002; 99:473–478. [PubMed: 11773633]

Nag TC, Wadhwa S. Differential expression of syntaxin-1 and synaptophysin in the developing and adult human retina. J Biosci. 2001; 26:179–191. [PubMed: 11426054]

Ng L, Hurley JB, Dierks B, Srinivas M, Salto C, Vennstrom B, Reh TA, Forrest D. A thyroid hormone receptor that is required for the development of green cone photoreceptors. Nat Genet. 2001; 27:94–98. [PubMed: 11138006]

Okada M, Erickson A, Hendrickson A. Light and electron microscopic analysis of synaptic development in Macaca monkey retina as detected by immunocytochemical labeling for the synaptic vesicle protein, SV2. Journal of Comparative Neurology. 1994; 339:535–558. [PubMed: 8144745]

Osterberg GA. Topography of the layer of rods and cones in the human retina. Acta Ophthalmologica. 1935; 13(Suppl 6):1–97.

Petry HM, Erichsen JT, Szel A. Immunocytochemical identification of photoreceptor populations in the tree shrew retina. Brain Research. 1993; 616:344–350. [PubMed: 8358626]

Provis JM, van Driel D, Billson FAB, Russell P. Development of the Human Retina: Patterns of cell distribution and redistribution in the ganglion cell layer. Journal of Comparative Neurology. 1985; 233:429–451. [PubMed: 3980779]

Provis JM. Patterns of cell death in the ganglion cell layer of the human fetal retina. Journal of Comparative Neurology. 1987; 259:237–246. [PubMed: 3584558]

Provis JM, Diaz CM, Dreher B. Ontogeny of the primate fovea: a central issue in retinal development. Progress in Neurobiology. 1998; 54:549–580. [PubMed: 9550191]

Raymond PA, Rivlin PK. Germinal cells in the goldfish retina that produce rod photoreceptors. Developmental Biology. 1987; 122:120–138. [PubMed: 3596007]

Reh TA, Fischer AJ. Retinal stem cells. Methods Enzymol. 2006; 419:52–73. [PubMed: 17141051]

Rodieck, RW. First Steps in Seeing. Sinauer; Sunderland, MA: 1998.

Swain PK, Hicks D, Mears AJ, Apel IJ, Smith JE, John SK, Hendrickson A, Milam AH, Swaroop A. Multiple phosphorylated isoforms of NRL are expressed in rod photoreceptors. Journal of Biological Chemistry. 2001; 276:36824–36830. [PubMed: 11477108]

van der Spuy J, Kim JH, Yu YS, Szel A, Luthert PJ, Clark BJ, Cheetham ME. The expression of the Leber congenital amaurosis protein AIPL1 coincides with rod and cone photoreceptor development. Invest Ophthalmol Vis Sci. 2003; 44:5396–5403. [PubMed: 14638743]

van Driel D, Provis JM, Billson FA. Early differentiation of ganglion, amacrine, bipolar and Müller cells in the developing fovea of human retina. Journal of Comparative Neurology. 1990; 291:203–219. [PubMed: 2298931]

Wilson JH, Wensel TG. The nature of dominant mutations of rhodopsin and implications for gene therapy. Mol Neurobiol. 2003; 28:149–158. [PubMed: 14576453]

Xiao M, Hendrickson A. Spatial and temporal expression of short, long/medium, or both opsins in human fetal cones. Journal of Comparative Neurology. 2000; 425:545–559. [PubMed: 10975879]

Yuodelis C, Hendrickson A. A qualitative and quantitative analysis of the human fovea during development. Vision Research. 1986; 26:847–855. [PubMed: 3750868]

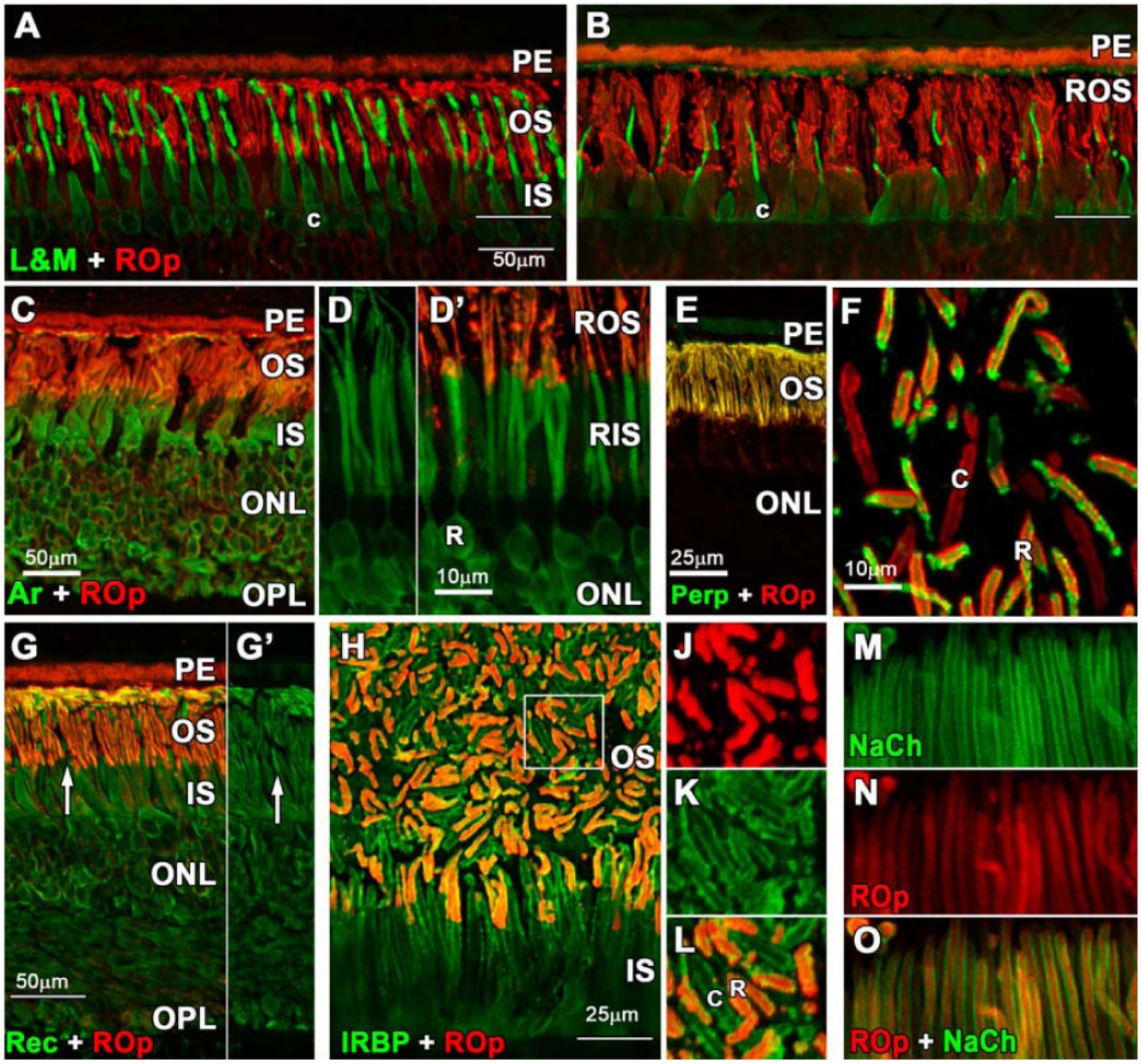

Figure 1.

Photomicrographs of adult human retina immunolabeled with antibodies to rod opsin (ROp, red), L&M cone opsin (L&M; green); rod arrestin, peripherin, recoverin, interphotoreceptor retinoid binding protein (IRBP) and the rod GTP-gated sodium channel (NaCh). **A-B.** L&M immunoreactive (IR) cones are more numerous and their outer segments (OS) longer in central (A) vs peripheral (B) retina. In central retina the ROp-IR rod OS (red) and L&M cone OS (green) are similar in length. In peripheral retina, cone OS are about half the length of rod OS. White line indicates the external limiting membrane. (Scale bars are 50 μm) **C-D′**. Arrestin is expressed throughout the rod cytoplasm (C,D) including the synaptic spherules, but arrestin labels the OS relatively lightly compared with ROp (D,D′). **E-F.** Perpherin is expressed in both rod and cone OS but not the cytoplasm (E). A tangential section shows

perpherin-IR cone (F, c) and ROp/Perp-IR rod OS. **G.** Recoverin is expressed throughout the cytoplasm of both cones (G,G′ white arrow) and rods with relatively light labeling of the OS. **H.** Double labeling for IRBP (green) and ROp (red) shows that this protein is located on the extracellular OS surface of both rods and cones. The region indicated by the box is shown at higher magnification for **J**: ROp, **K**: IRBP, **L**: ROp/IRBP. **M-O**. Rod OS have heavy labeling for NaCh in the surface membrane (M) while ROp more evenly labels the OS membrane and discs (N). Scale bars A-C; G = 50μm, D;F;J-K= 10μm, E;H =25μm.

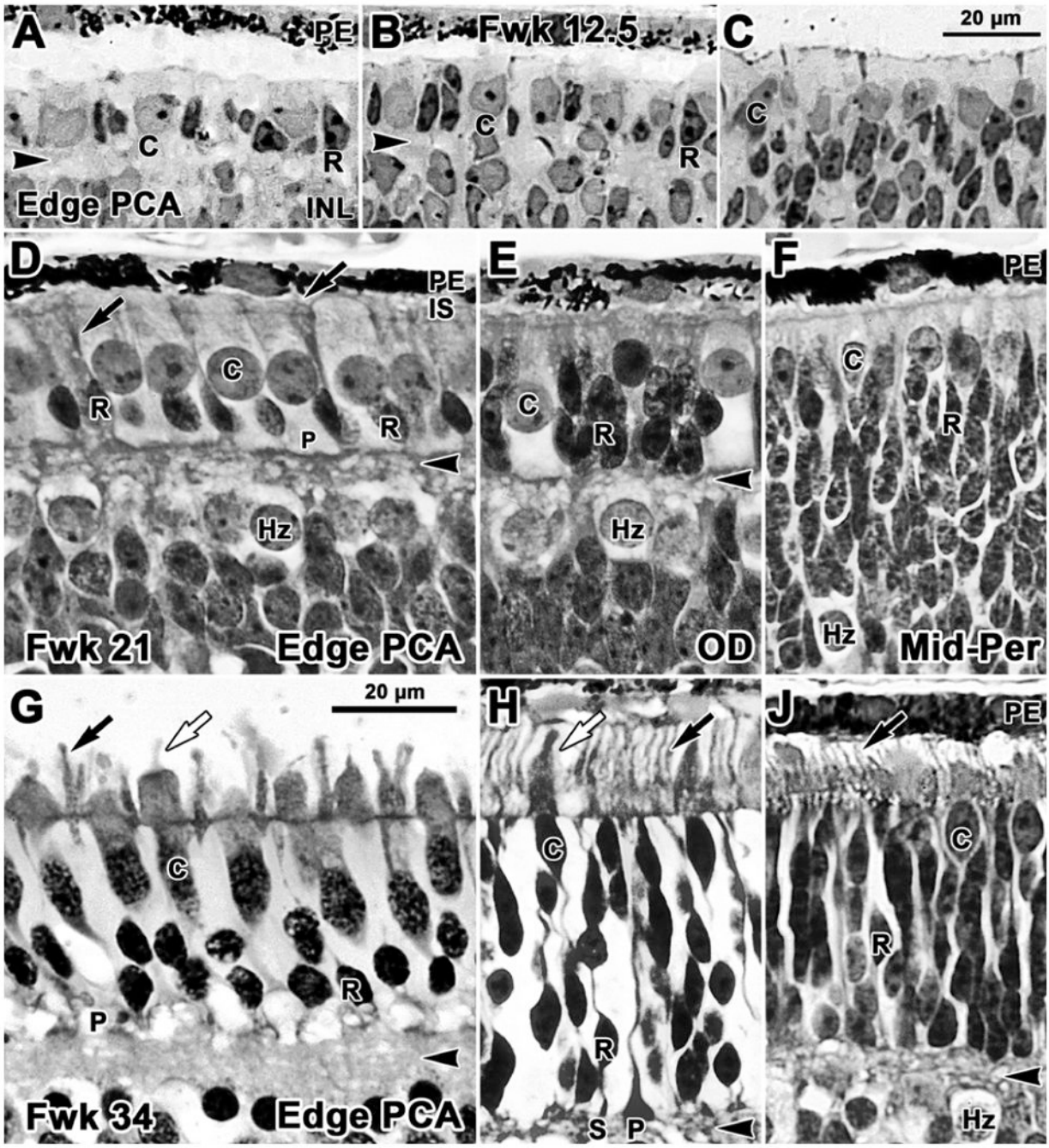

Figure 2.

Photomicrographs from glycol methacrylate sections of human retina stained with azure II & methylene blue. Sections are aligned on the external limiting membrane. **A-C** Fwk12.5; **D-F** Fwk21; **G-J** Fwk34. **A.** Rods (R) are present on the edge of the pure cone area (PCA), the site of the future fovea. Rods have elongated, densely stained nuclei and a tiny amount of dense cytoplasm in contrast to the pale larger cones (C). **B.** Rods and cones both are present 400µm further peripheral at the point where the outer plexiform layer (OPL; arrowhead) disappears. **C.** Only cones can be identified in more peripheral retina. **D.** Near

the developing fovea the smaller dense rod nuclei form a single row of cells adjacent to the OPL. The larger cone nuclei and cell bodies form a packed single layer and cone pedicles (P) line the outer border of the OPL. The inner OPL border is formed by a band of pale horizontal cells (Hz). Thin dense inner segments (IS; arrow) are present on rods. OS cannot be easily identified, although antibody labeling (see Fig.6) shows that they are present on both cones and rods. **E.** Temporal to the optic disk (OD) cones are sparse while rods are stacked 3-4 cells deep adjacent to the thin OPL. **F.** In midperipheral retina the OPL is not yet present. A single row of cones lines the outermost retina, while rods are stacked 10-12 cells deep and merge with pale Hz. **G.** Near the fovea, rods are 2 cells deep and have well developed IS and OS (black arrow). Cones have thick IS and short OS (white arrow). **H.** At the OD rods greatly outnumber cones. Compared to **G**, both rods and cones are more mature, have longer IS and OS and distinct synaptic spherules (S) and pedicles (P). **J.** A thin OPL is present in the midperiphery and rods are stacked 9-12 cells deep under the cones. Both rods and cones have short IS and OS (arrow). Scale bar in C for A-C; in G for D-J.

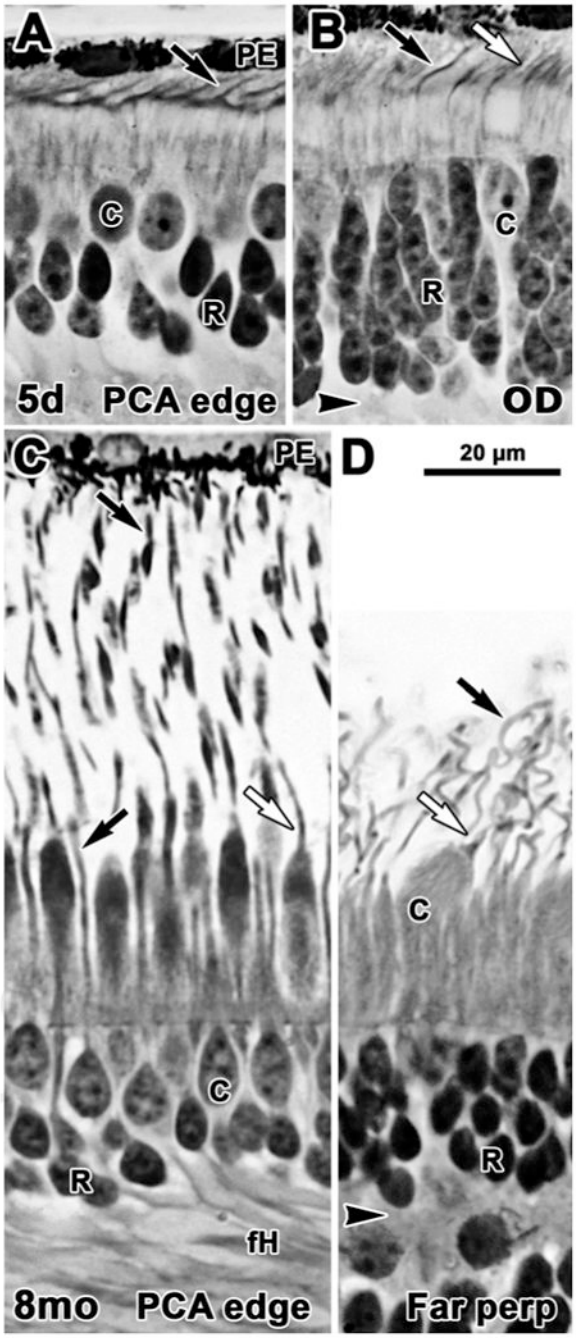

Figure 3.

Photomicrographs from glycol methacrylate sections of human postnatal retina. Sections are aligned on the external limiting membrane. **A-B** 5 days; **C-D** 8 months. **A**. Near the PCA rods are 2-3 deep with distinct OS present on both rods (arrow) and cones. **B.** Near the OD rods are 5-6 cells deep and both rods (black arrow) and cones (white arrow) have significantly longer IS and OS than those on the edge of the fovea. **C.** Rod (black arrow) and cone (white arrow) OS on the PCA edge are much longer than in the newborn. Photoreceptors in and around the fovea have also elaborated long basal axons (fH),

increasing the thickness of the OPL. **D.** Very long, thin rod OS and shorter, thicker cone OS are present well into the periphery. Scale bar in D for A-D.

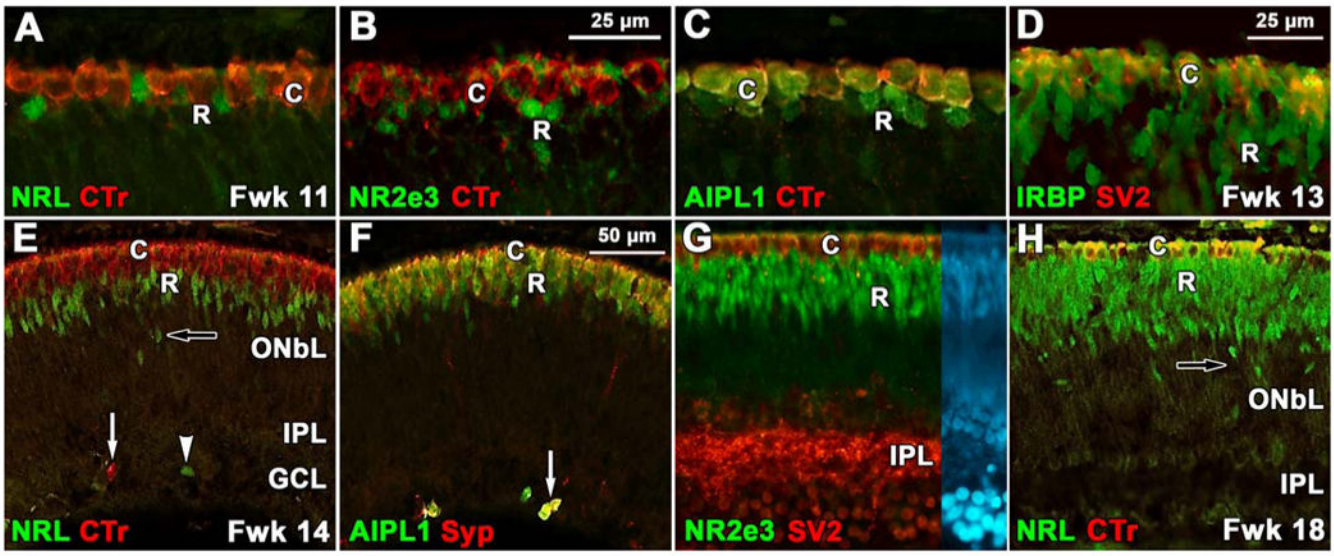

Figure 4.

Expression of the early group of rod proteins. **A-C**: Edge of the PCA at Fwk 11. **A**: Cone cytoplasm (C) labels for cone transducin (CTr, red) while the underlying rod nuclei (R) are NRL-IR (green). **B**: NR2e3 labels rod nuclei (green) which is clearly distinguishable from the transducin-IR cytoplasm (red) of the cones. **C**: Cone cytoplasm double labels for AIPL1 and transducin (yellow) while the rods are only labeled for AIPL1 (green). **D**: At Fwk13 central cones are double labeled for IRBP and synaptic vesicle protein 2 (SV2, yellow) while rods label only for IRPB (green). **E-G**: Fwk 14-15. **E**: In the midperiphery, a band of NRL-IR rod nuclei (green) 3-5 cells deep are found on the inner aspect of a single layer of transducin-IR cones (red). Transducin (arrow) and NRL-IR (arrowhead) cells are also present in the inner retina. **F**: Cones are double labeled (yellow) for AIPL1 and synaptophysin (Syp; red) while the deeper rods are AIPL1-IR only (green). A group of single and double labeled cones in inner retina is indicated (arrow). **G**: In peripheral Fwk15 retina, SV2-IR cones (red) and NR2E3-IR rod nuclei (green) form distinct bands in the outer retina. Note the heavy SV2 labeling in the IPL, but the absence of a distinct OPL. Right side of image shows nuclear (DAPI) labeling in the same section. **H**: In the Fwk18 midperiphery the layer of NRL-IR rod nuclei (green) is twice as thick as Fwk14 (**E**) with scattered NRL-IR nuclei lying much deeper in the retina (arrow). The cone cytoplasm, but not the nucleus, labels for both transducin and NRL at this age (see Swain et al.,2001; yellow). Scale bar in B for B-C; in D for D, G; in F for E,F,H

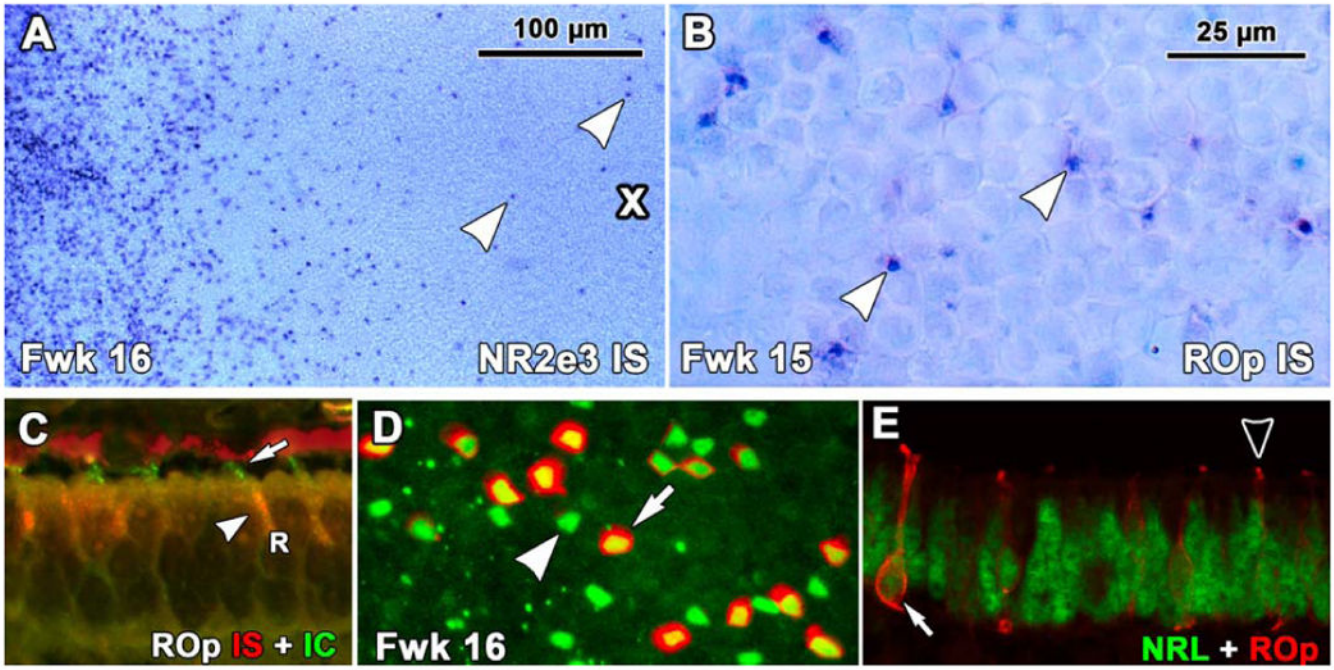

Figure 5.

Expression of rod opsin (ROp) mRNA as detected by insitu hybridization (IS) in human fetal retina. **A.** A Fwk16 wholemount hybridized to detect NR2E3 mRNA around the PCA (cross). The PCA is surrounded by a thick band of NR2E3 expressing rods with scattered NR2E3 expressing rods within the PCA (arrowheads). **B**. ROp mRNA is first expressed in scattered rods on the edge of the PCA (arrowheads) **C.** Fwk16 section processed first for ROp mRNA (red) and then for ROp protein (green). Rods have red IS (arrowheads) and short green OS (arrow). **D**: A Fwk16 wholemount at the edge of ROp expression double labeled for NRL (green) and ROp protein (red). Note the large number of single labeled NRL-IR nuclei (arrowhead) with NRL/ROp-IR rods scattered in between (arrow). **E**, A Fwk16 section at the front of ROp expression. The arrow indicates a rod with a NRL-IR nucleus (green) which is outlined by ROp-IR membrane (arrow, red). Most other adjacent rods have either NRL-IR nuclei only or a tiny ROp-IR OS (arrowhead). Scale bar in B for B-E.

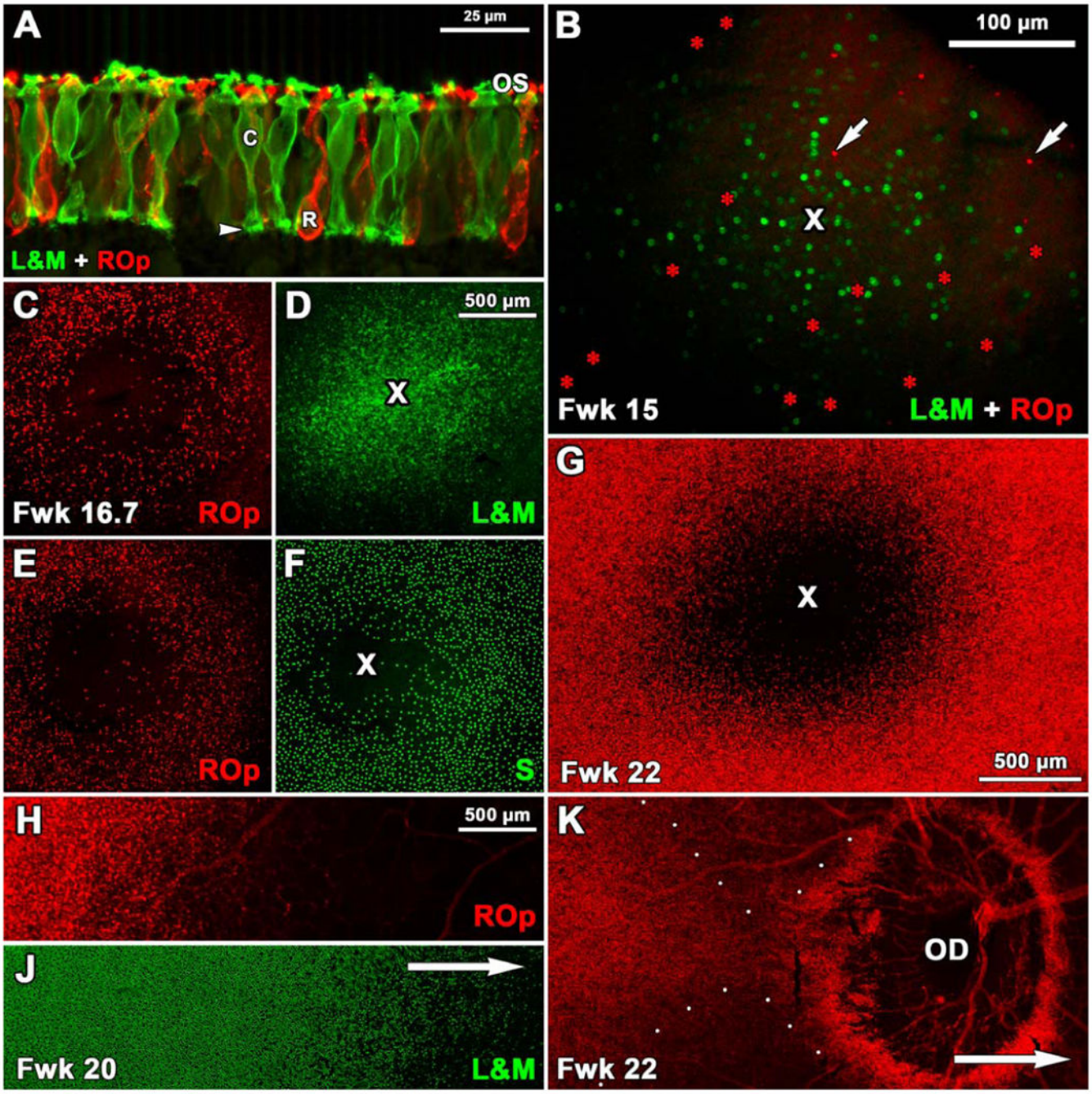

Figure 6.

Expression of ROp, L&M and S opsin in fetal human retina. **A**: A section through the PCA edge at Fwk 18 shows many ROp-IR rods (red) and L&M-IR cones (green). The entire photoreceptor cell membrane including the synaptic pedicle of cones (arrowhead) is labeled. Short OS are present on both rods and cones. **B**. Fwk15 wholemount showing 262 L&M-IR (green) cones and 37 ROp-IR (red, arrows) rods present in or around the PCA (cross). **C-F**: Two retinal wholemounts from the same Fwk16.7 fetus. ROp labeling (**D,F**, red) shows a 680µm wide PCA which not entirely “rod-free”. The future foveal center is packed with

L&M-IR cones (**E**, cross) and is surrounded by a dense ring of S-IR cones which are sparse in the PCA center (**F**, cross). **G**: By Fwk 22 the PCA is almost completely rod free, and is surrounded by densely packed ROp-IR rods. **H-J.** Double labeled Fwk 20 wholemount showing the relative position for the fronts of ROp (J) and L&M (K) expression. Arrow indicates direction of the optic disc (OD). **K**: Wholemount showing precocious ROp expression (red). Although the main expression front (to the left) has not reached the OD, many ROp-IR rods surround it. ROp-IR rods are absent peripheral to the OD (direction of arrow). Scale bar in D for C-F; in H for H-K.

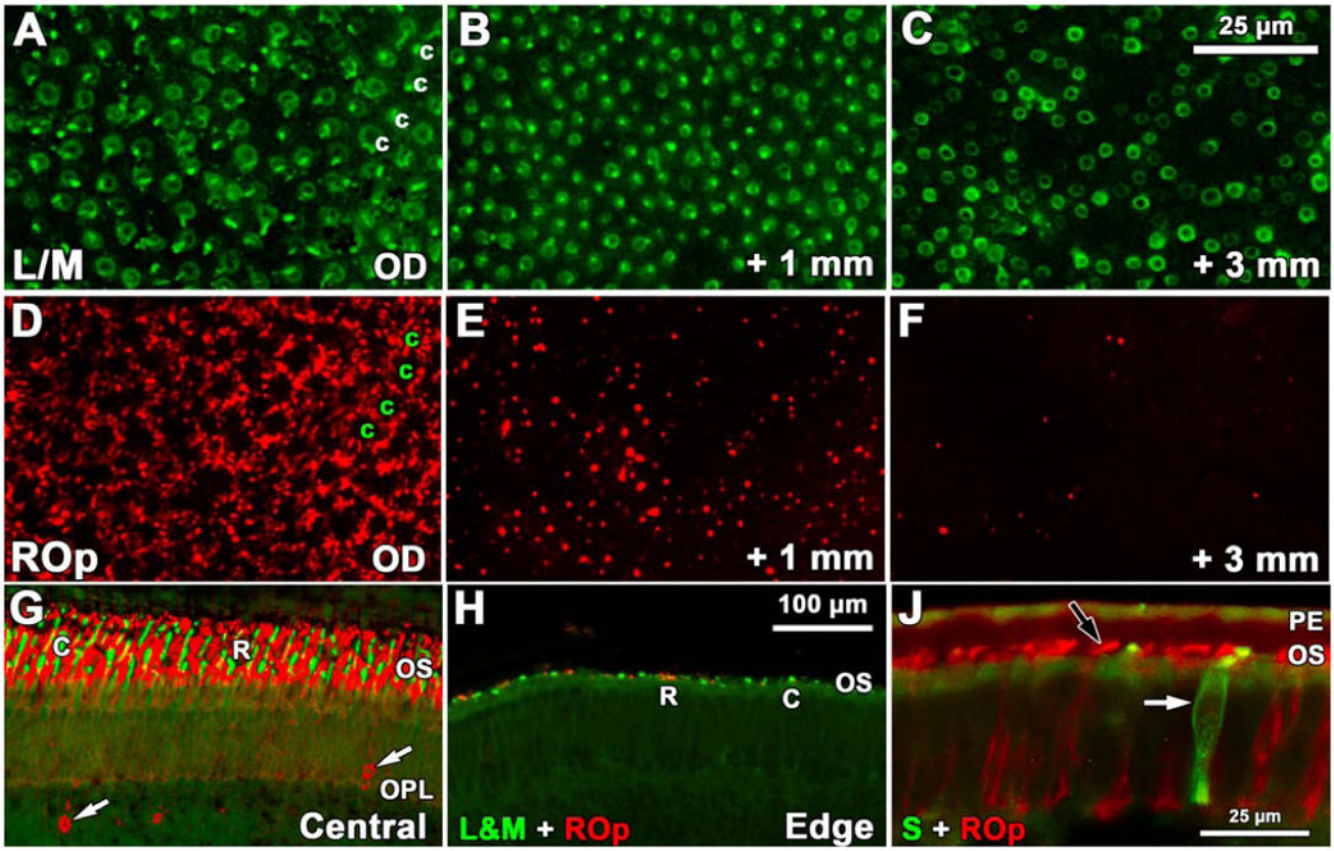

Figure 7.

Development of rod and cone opsin labeling in late fetal and neonatal human retina. **A-F**: Fwk 25 wholemount showing the pattern and relative number of L&M-IR cones (**A-C**) and ROp-IR rods (**D-F**) near the optic disc (**A,D**), 1mm (**B,E**) and 3mm (**C,F**) peripheral to the optic disc. A,D. Near the optic disc L&M-IR cones (A, c) are encircled by a dense rim of ROp-IR rods (D) in a mature pattern, suggesting that all photoreceptors have expressed opsin. **B, E**. At 1mm peripheral to the optic disc the L/M-IR cone pattern (B) has a few regions lacking cones, but rod density has dropped markedly (E). **C,F.** At 3mm there are fewer L/M-IR cones (C) although they can be identified at least several mm more peripherally. Rods (F) are very sparse at 3mm **G-H**. A comparison of ROp and L/M labeling in central retina (**G**) and near the retinal edge (**H**) at P1day. The neonatal central retina has long cone (c; green) and rod (r; red) OS while both are sparse and very short at the retinal edge. The central retina has many ROp-IR ectopic cells in inner retina (arrows). **J**: A comparison of ROp-IR (black arrow) rods and S opsin-IR cones (white arrow) in the periphery of the 5day retina. Scale bar in C for A-F; bar in H for G-H.

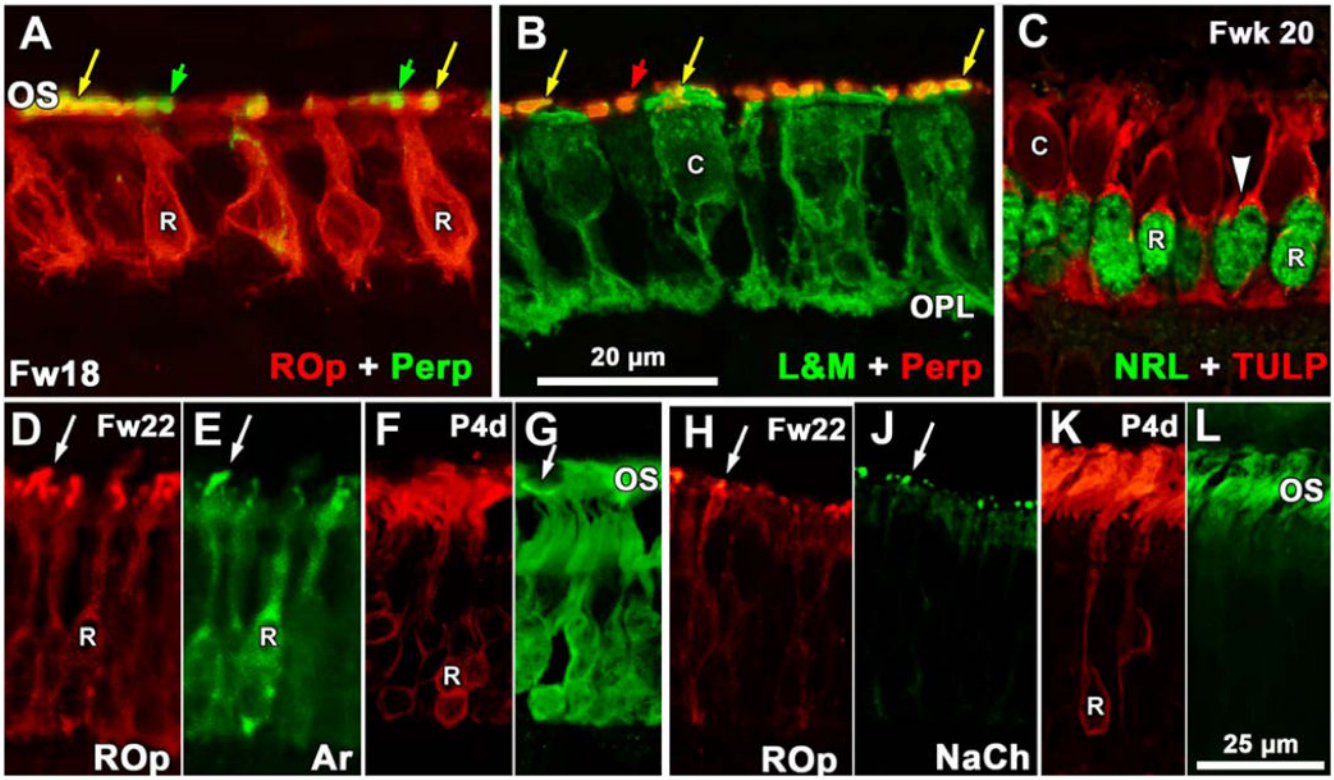

Figure 8.

Expression of phototransduction and OS structural proteins. **A-B**. Sections near the Fwk18 PCA. **A** shows rods double-labeled for peripherin (perp; green) and ROp (red) while **B** shows cones double labeled for L&M (green) and peripherin (perp; red). Both rod and cone OS are double labeled (yellow arrows) while peripherin-IR cone OS (A, green arrows) and rod OS (B, red arrows) are intermixed. Perpipherin label in cell bodies is minimal. Note that rods lack any obvious synaptic spherule but cones have a well developed pedicle in the OPL. **C**: Section of Fwk20 retina near the PCA edge showing the appearance of TULP (red) in rods which have an NRL-IR nucleus (green). A thin rim of TULP-IR cytoplasm (arrowhead) marks the rods. Cone cytoplasm is also TULP-IR but OS do not label. **D-E**: Fwk22 rods OS double label for ROp (**D**) and rod arrestin (**E**). Both the cell membrane and short OS (arrow) double label. **F-G**. Postnatal 4day rods have mainly OS label for ROp (**F**) with heavy cytoplasmic and lighter OS labeling for arrestin (**G**). The arrow indicates an arrestin-IR S cone OS. **H-J.** Most of the short Fwk22 rod OS (arrows) are double labeled for ROp and NaCh. **K-L**. Rod OS labeling has increased at 4days for ROp (K) and NaCh (L) with little cytoplasmic labeling for either protein. Magnification bar in B for A-B; bar in L for D-L.

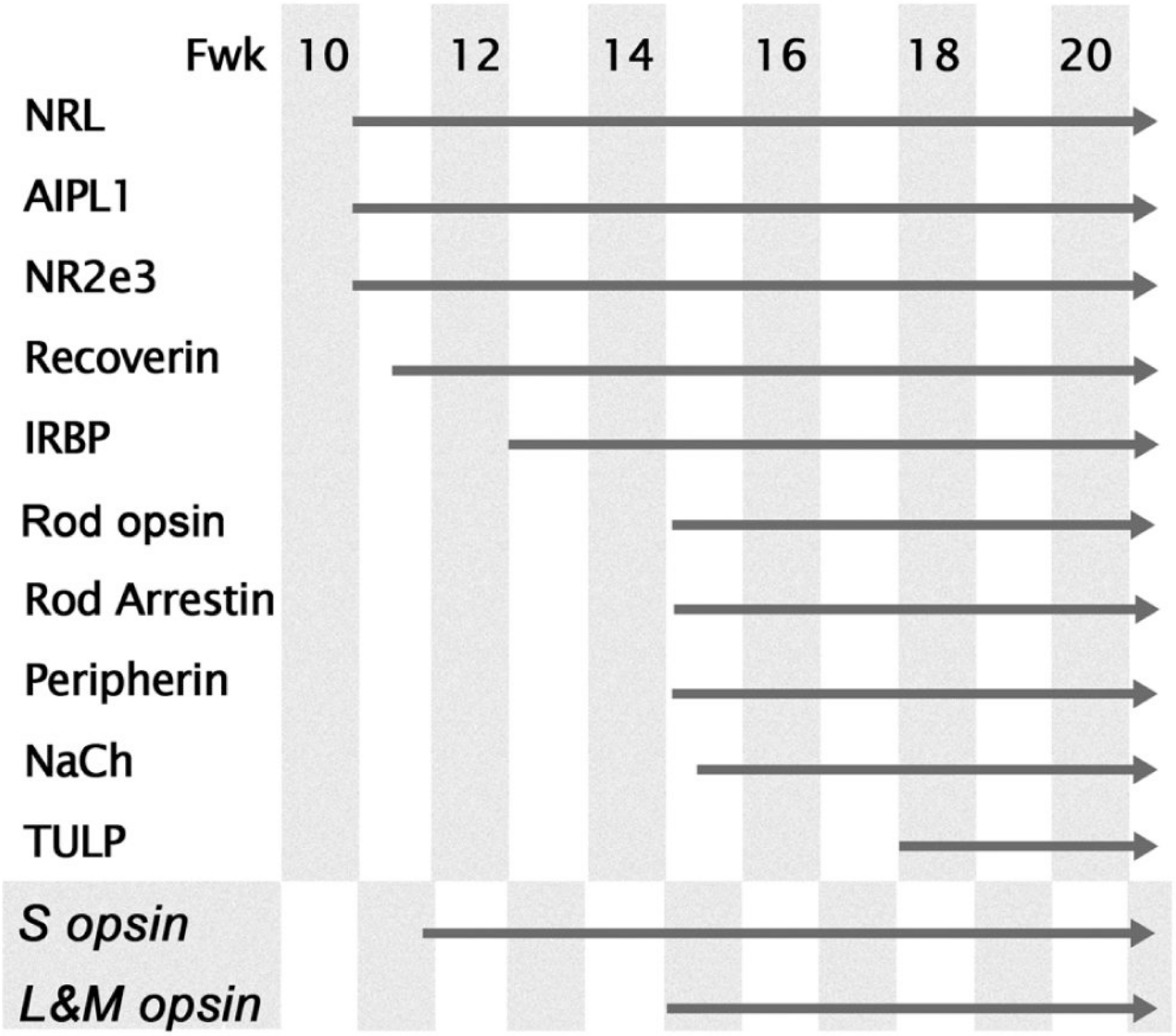

Figure 9.

Expression sequence of proteins in rods on the edge of the PCA. Cone opsins are included for comparison. Note the early group of NRL, AIPL1, NR2e3, recoverin and IRBP appear 3-5 weeks before rod opsin. The phototransduction associated proteins, peripherin, rod arrestin, and NaCh, are expressed at the same time or soon after rod opsin with TULP the last to appear in rods.